THE JOURNAL OF PHYSICAL CHEMISTRY A

Article

Excited-State Molecular Dynamics Triggered by Light Pulses – Ab Initio Multiple Spawning vs Trajectory Surface Hopping

Benoit Mignolet, and Basile F. E. Curchod

J. Phys. Chem. A, **Just Accepted Manuscript** • DOI: 10.1021/acs.jpca.9b00940 • Publication Date (Web): 02 Apr 2019

ACS Publications

is published by the American Chemical Society. 1155 Sixteenth Street N.W., Washington, DC 20036

Excited-State Molecular Dynamics Triggered by Light Pulses – Ab Initio Multiple Spawning vs Trajectory Surface Hopping

Benoit Mignolet[†] and Basile F. E. Curchod[*,‡]

[†]*Theoretical Physical Chemistry, UR MolSYS, B6c, University of Liège, B4000 Liège, Belgium*

[‡]*Department of Chemistry, Durham University, South Road, Durham DH1 3LE, United Kingdom*

E-mail: basile.f.curchod@durham.ac.uk

Abstract

Trajectory surface hopping and *ab initio* multiple spawning are two commonly employed methods for simulating the excited-state dynamics of molecules. Trajectory surface hopping portrays the dynamics of nuclear wavepackets by a swarm of independent classical trajectories, which can *hop* between electronic states. *Ab initio* multiple spawning, on the other hand, expresses nuclear wavepackets in a basis of traveling, coupled basis functions, whose number can be extended in case of coupling between electronic states. In the following, we propose to compare the performance of these two methods to describe processes involving the explicit interaction of a molecule with laser pulses. We base this comparison on the LiH molecule, as it is compatible with numerically-exact simulations using quantum dynamics. As recognized in earlier works, the limitations of TSH due to its inherent independent trajectory approximation are further enhanced when studying an explicit photoexcitation. While *ab initio* multiple spawning is also based on a series of approximations, the couplings between its traveling basis functions allow for a proper description of phenomena that TSH cannot describe with its inherent independent trajectory approximation, even when applying decoherence corrections. We show here for different *in silico* experiments involving laser pulses that *ab initio* multiple spawning overcomes the limitations experienced by trajectory surface hopping and offers an at least qualitative description of population transfer between electronic states.

Introduction

Over the last decades, an impressive amount of work has been invested in the development of theoretical strategies to describe the dynamics of molecules in their excited electronic states.[1–3] Such theoretical surge has not only been stimulated by the curiosity of investigating molecular processes beyond the famous Born-Oppenheimer approximation, but also by advancement in experimental techniques like femto- and attosecond spectroscopy and the

increasing use of light-triggered processes in chemical applications related for example to renewable energies, bioimaging, or chemical synthesis.

The very first step of a photochemical and photophysical process consists of the absorption of a photon by the molecule of interest. The molecular state resulting from this photoexcitation process will significantly vary depending on the characteristic of the electromagnetic radiation applied onto the molecule.[4–6] From a theoretical perspective, it is often assumed that a molecule is initially in its ground electronic (and vibrational) state and will interact with a very short pulse of light, forming a nuclear wavepacket on a given excited electronic state. Within this assumption, the photoexcitation process can be neglected and the excited-state dynamics simulations simply initialized by launching a nuclear wavepacket directly from a selected excited electronic state.

Several methods have been devised to treat the excited-state dynamics of molecules following photoexcitation, as well as the nonadiabatic effects encountered when the Born-Oppenheimer approximation breaks down. These strategies mostly differ on the accuracy they achieve to describe the quantum nature of the nuclei and the electron-nuclear coupling. An accurate description of the nuclear wavepacket dynamics can be obtained by employing a numerical grid and static basis functions,[7–9] or by using traveling basis functions[10] as done in variational Multiconfiguration Gaussian (vMCG),[11–16] multiconfiguration Ehrenfest (MCE)[17–20] or Full Multiple Spawning (FMS).[21–27] At a more approximate level, mixed quantum/classical methods propose to approximate the description of nonadiabatic transitions while using a classical approximation for the nuclei.[28,29] Trajectory surface hopping (TSH),[30–32] Ehrenfest dynamics,[28,33,34] or more recent methods like the Coupled Trajectory Mixed-Quantum Classical approach[35–38] are all examples of mixed quantum/classical techniques.

Nonadiabatic dynamics techniques can also be extended to account for the coupling of a molecule with the external electromagnetic field, allowing for an explicit simulation of the initial photoexcitation process mentioned above. Among the different strategies pro-

posed, light-triggered excited-state dynamics of molecules in their full configuration space has been achieved TSH,[39–47] Ehrenfest dynamics,[48] and more recently by employing *ab initio* nonadiabatic quantum dynamics methods like *ab initio* multiple spawning (AIMS)[49–51] or *Ab Initio* Multiple Cloning.[52] Whereas TSH is one of the most commonly employed technique for nonadiabatic molecular dynamics, the validity of its approximations to describe light-triggered phenomena has been severely questioned, with no clear strategy to fix TSH issues.[44] The recent extension of FMS to include a coupling with an external field, coined XFFMS (eXternal Field FMS), offers an alternative strategy to TSH for simulating light-induced phenomena. In particular, its approximate form, XFAIMS (eXternal Field *Ab Initio* Multiple Spawning)[51] opens the door for the simulation of molecular systems of the same size as in TSH.[53] In a previous work, we proposed a detailed test of the different approximations linking the *in-principle* exact XFFMS to XFAIMS for photoexcitation processes.[54] Here, we aim at validating the use of XFAIMS for the description of molecular photoexcitation by comparing it to TSH and numerically-exact quantum dynamics (QD) simulations. We show that XFAIMS, thanks to its use of coupled traveling basis functions, reproduces at least qualitatively the QD results for processes involving long or multiple pulses, which otherwise leads to a breakdown of the TSH approximations.

In the following, we start by discussing the formalism of XFAIMS and TSH, with a focus on the explicit description of light-induced excitation processes in a molecule. We then conduct three *in silico* experiments with XFAIMS and TSH, where we excite the molecule LiH with different laser pulses. These simulations aim at stressing the approximations of TSH and XFAIMS, and their outcomes are compared with those of numerically-exact QD.

Theory

We propose here a brief introduction to FMS, AIMS, and TSH in the context of nonadiabatic dynamics including an external electromagnetic field. The interested reader is referred to

Ref. 10 for a general review on AIMS, including a comparison of its formalism with that of TSH, and Ref. 29 for a presentation of TSH and its different flavors.

Full- and *Ab Initio* Multiple Spawning

The idea behind FMS[21–24,26] is to expand the nuclear wavefunctions evolving in each electronic state in a basis of *moving* basis functions. More precisely, the nuclear wavefunction in a given electronic state is represented by a linear combination of Gaussians with a frozen width, called trajectory basis functions (TBFs). These TBFs are not fixed in space but evolve in the corresponding electronic state according to classical equations of motion – the TBFs hence form a sort of moving grid that offers at all time of the simulation a proper support to describe the nuclear wavefunction. When a TBF evolving in electronic state J reaches a region of strong nonadiabaticity with a different electronic state I, new TBFs are *spawned* on the coupled state I such that amplitude can be transferred from one state to the other as a result of the nonadiabatic transition (details of the spawning algorithm can be found in Refs. 10,26). Importantly, all TBFs are *coupled* together *via* the time-dependent Schrödinger equation, and can, therefore, exchange amplitude (both in an intra- and an interstate manner). In this sense, FMS is *in principle* exact when a large number of TBFs is employed, as discussed in Ref. 54.

FMS is in principle exact, but the numerically-exact calculation of the integrals necessary to couple the TBFs requires to know the potential energy surfaces and nonadiabatic coupling terms over the entire molecular configuration space,[54] making the method intractable for molecular systems. Two approximations can be deployed to simplify these integrals: (i) the saddle-point approximation (SPA), where the nuclear-coordinate dependence of the electronic structure quantity in the integrand is approximated by a truncated Taylor expansion at the centroid position of the two TBFs, and (ii) the independent first generation approximation (IFGA), where the initial (parent) TBFs describing the nuclear wavefunction (or wavepacket) at time $t = 0$ are considered uncoupled. Applying these two approximations to

the FMS framework allows for the calculation of all necessary electronic-structure quantities on-the-fly, and the resulting method is called *Ab Initio* Multiple Spawning, AIMS. The effects and robustness of these approximations have recently been tested.[54]

Including explicitly the coupling between a molecule and an external electromagnetic field (like a laser pulse) is straightforward within the FMS framework: a light/matter interaction Hamiltonian (or dipolar coupling interaction term – coupling between the external electromagnetic field and the molecular dipole moment of the molecule) can be added to the molecular Hamiltonian, leading to new couplings between TBFs as a result of the external electromagnetic field.[51] The spawning algorithm can be adapted to ensure an adequate creation of TBFs in the coupled electronic states when the electromagnetic radiation is switched on. XFFMS (or XFAIMS, within the SPA and the IFGA), allows for the explicit simulation of the photoexcitation process of a molecule, from its ground electronic state, by an external electromagnetic field.[51] In a typical XFAIMS run (upper panel of, Fig. 1), a parent TBF is initiated at time t_0 in the ground electronic state, the XFAIMS dynamics starts, and the coupling between the external electromagnetic field and the molecule at later times (t') will trigger the spawning of new TBFs to the coupled electronic state (here S_1), and possibly also in the ground state (not depicted in Fig. 1 for clarity). The creation of new TBFs will allow for both intra- and interstate amplitude transfer between all TBFs (blue and green arrows in Fig. 1, on the upper right panel). Once the termination criterion of the dynamics is reached, another run can be initiated from a different initial (parent) TBF in the ground state. Any properties of interest are then averaged incoherently over all the XFAIMS runs performed.[10,26]

Trajectory Surface Hopping

Trajectory surface hopping is a mixed quantum/classical method[29] that pictures the dynamics of nuclear wavepackets by swarms of independent classical trajectories. These trajectories are propagated adiabatically in the electronic state of interest and can *hop* between electronic

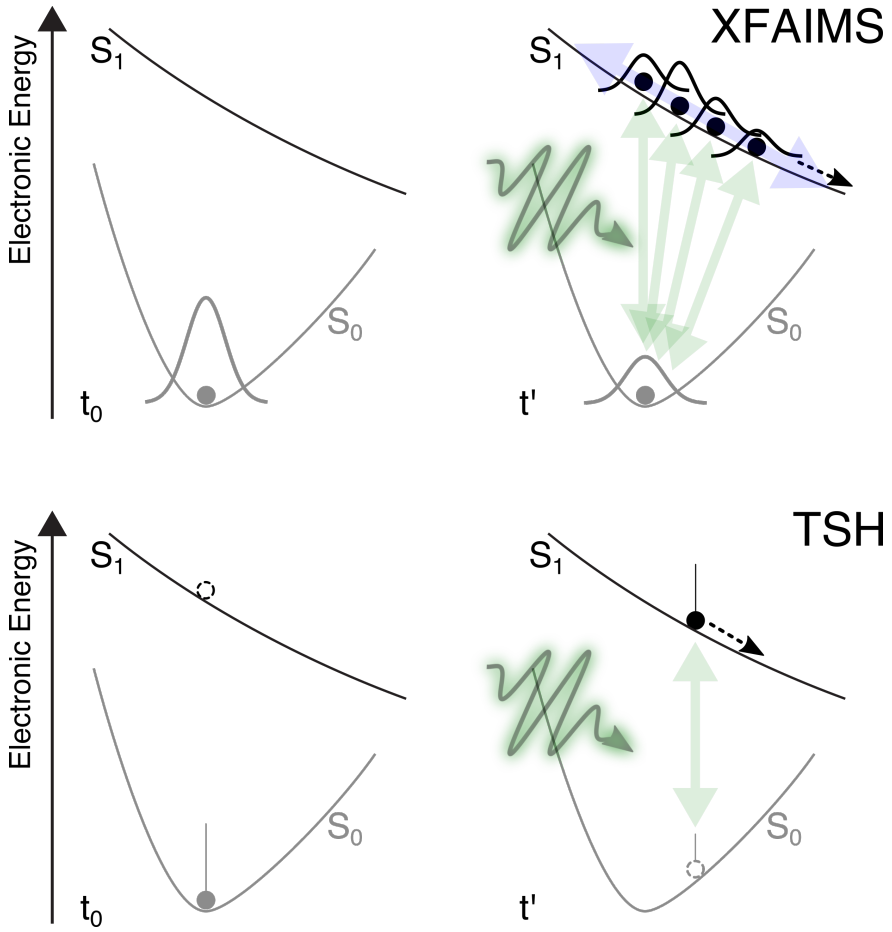

Figure 1: Schematic representation of a photoexcitation process as pictured by XFAIMS (upper panel) or TSH (lower panel) at initial time (t_0) and during the interaction with the laser pulse (t'). The TBFs in AIMS (upper panel) are depicted as Gaussians (with their center moving according to classical equations of motion) and are coupled together *via* intrastate (blue arrow) and interstate coupling (green arrows) terms. In TSH (lower panel), the trajectory driving the dynamics is indicated by a filled circle (in S_0 at time t_0), while the "ghost" trajectory (in S_1 at time t_0), which follows the driving trajectory, is given by a dashed circle. The bar on top of each trajectory symbolizes the amount of amplitude carried by each state. Due to the independent classical trajectory approximation, only the amplitudes following one single trajectory are connected via the laser pulse. See text for more information.

states whenever they reach regions of strong nonadiabatic coupling. The idea of TSH was proposed around the seventies,[30,31] but the hopping algorithm commonly employed nowadays was devised by Tully in 1990 and is called 'fewest switches'.[32] In short, a typical TSH run works as follows: an independent trajectory is initiated in a selected excited electronic state, and a set of complex amplitudes is attached to this trajectory. At the beginning of

the dynamics, the amplitude corresponding to the driving state is set to 1, while all the other amplitudes remain zero. The molecule evolves on the potential energy surface (PES) corresponding to the initial electronic state, and the amplitudes are propagated along this trajectory based on an electronic time-dependent Schrödinger equation. After each nuclear time step, the fewest-switches algorithm dictates stochastically if the trajectory has to remain on this electronic state, or to hop to another one. If the molecule reaches a region of strong nonadiabaticity, some amplitude can be transferred from the driving state to the coupled state: the combination of an increase in nonadiabatic coupling strength with an exchange of amplitude between states will increase the probability for the trajectory to hop to the coupled state. The trajectory is propagated until a certain predefined criterion is reached. This full sequence is repeated for many independent trajectories until convergence of the quantity of interest is reached. Importantly, 'convergence' here does not necessarily mean convergence to the exact result, as fewest-switches TSH is an approximate method that cannot be straightforwardly derived from first principles.[32,55,56] Nevertheless, TSH has been successfully employed to study the nonadiabatic dynamics of several molecules in their full dimensionality.[57]

As discussed in several references,[45,55,58–64] the independent trajectory approximation is the reason for the simplicity and efficiency of the TSH algorithm, but it also constitutes the Achille's heel of this method. This approximation implies that the TSH amplitudes are propagated on the support of a single trajectories, meaning that when electronic states differ substantially in their respective PESs, TSH amplitudes cannot *decohere*. By decoherence, one means here that nuclear wavepackets formed on different PESs after a coupling region are likely to move away from each other. Within the independent trajectory approximation of TSH, the amplitudes of all electronic states are forced to follow the single classical trajectory in its dynamics along the selected electronic state: they cannot decohere, and any subsequent interaction between these amplitudes at later times might lead to artifacts in the dynamics. Different methods have been devised to correct for this overcoherence effect,[59,60,65–70] and

operate for example by decaying the amplitude on the states not driving the dynamics.

Different strategies were proposed to include the effect of an explicit external electromagnetic field in fewest-switches TSH. One possibility is to add a dipolar coupling interaction term in the electronic Hamiltonian used to propagate the TSH amplitudes. The fewest-switches can be adapted to account for this new source of couplings between electronic states.[40,42] This strategy can be called field-diabatic TSH, as it employs the bare adiabatic electronic states for the nuclear dynamics. Another technique proposes to include the effect of the external electromagnetic field directly in the PES, by adiabatizing the electronic states and their couplings *via* the dipolar coupling interaction term.[71–74] The latter proposal is based on the observation that TSH operates better in the adiabatic representation of the electronic states, where coupling terms are localized in space.[72] Finally, TSH can be transferred to a Floquet picture[47] or use local-diabatization.[44]

The lower panel of Fig. 1 depicts schematically the dynamics of a single TSH trajectory (in a field-diabatic picture). The trajectory driving the dynamics is indicated by a filled circle (in S_0 at time t_0), while the "ghost" trajectory on S_1, which follows the driving trajectory, is given by a dashed circle. The bar on top of each trajectory indicates the amount of amplitude carried by each electronic state, which is 1 for S_0 at t_0 (long bar). When the laser pulse reaches the molecule, amplitude is transferred to the S_1 state (pictorially represented by smaller bars). This transfer of amplitude can lead to a hop of the classical trajectory towards S_1, which will now drive the dynamics (t'). Due to the independent classical trajectory approximation, only the amplitudes following one single trajectory are connected via the laser pulse. The decoherence problem of TSH is expected to be exacerbated when studying the photoexcitation of a molecule by an external electromagnetic,[44,45] as a result of the differences in PESs shape between the ground and the excited electronic states in the direct vicinity of the Franck-Condon region. This issue can be conceptualized by the schematic picture introduced in Fig. 1: at t', the TSH trajectory evolves on S_1 and carries its S_1 amplitude (black bar). However, the amplitude of S_0 is constrained to follow the driving

trajectory, as if the ghost trajectory was going up the S_0 potential while it should, in fact, remain in the Franck-Condon region. The effect of a decoherence correction, in this particular case, would be to reduce the residual amplitude on S_0 at later times (when the dynamics is driven by S_1), as discussed below for the case of an ultrashort UV pulse.

Computational details

In all the simulations presented below, we used Gaussian-shaped pulses, $\underline{\boldsymbol{E}}(t)$, defined from the time derivative of the vector potential:

$$\underline{\boldsymbol{E}}(t) = -\frac{1}{c}\frac{d\underline{\boldsymbol{A}}(t)}{dt} \tag{1}$$

with

$$\underline{\boldsymbol{A}}(t) = \underline{\boldsymbol{\epsilon}}\frac{cf_0}{\omega}\exp\left[-\frac{(t-t_0)^2}{2\sigma^2}\right]\sin(\omega t)\ . \tag{2}$$

In Eq. (2), $\underline{\boldsymbol{\epsilon}}$ is the polarization vector, c the speed of light, f_0 the field strength, ω the carrier frequency, and σ is related to the pulse duration. The full width at half maximum of the pulse is 2.35σ. In the next section, the LiH molecule will be photoexcited by (*i*) a single UV pulse, (*ii*) a single IR pulse, and (*iii*) a combination of two identical UV pulses in a pump-probe scheme. The UV pulses used are resonant with the S_0-S_1 transition of LiH ($\omega = 0.127$ a.u., 360 nm), polarized parallel to the molecular axis, have an intensity of $1.4 \cdot 10^{13}$ W/cm^2 ($f_0 = 0.02$ a.u.), and a duration of 71 a.u. ($\sigma = 30$ a.u.). By 'resonant', we mean here that the pulse has a carrier frequency that corresponds to the S_0/S_1 electronic energy difference at the ground-state equilibrium geometry. The IR pulse is less intense ($f_0 = 0.01$ a.u., $3.5 \cdot 10^{12}$ W/cm^2) and significantly longer ($\sigma = 500$ a.u., FWHM= 1175 a.u.) than the UV pulse, but is off-resonant ($\omega = 0.057$ a.u., 800 nm).

The numerically-exact QD simulations were carried out in the two lowest electronic states (S_0 and S_1) of LiH, on potential energy curves (PECs) computed at the SA2-CASSCF(4/6)/6-31G level of theory. The PECs were discretized on a grid, with the LiH bond distance varying

from 0.5 to 15.0 a.u. with a spacing of 0.02 a.u.. The dynamics starts from the ground state with an initial wavefunction that has been selected to mimic the ground vibrational eigenstate of LiH. In the simulations, we focus on the $S_0 \rightarrow S_1$ photoexcitation efficiency and subsequent excited-state dynamics, and will therefore not consider other possible photoexcitation processes to higher excited states as well as nonradiative relaxation (due to the very small nonadiabatic coupling terms between these states).

The XFAIMS simulations were performed in internal coordinates using the same PECs and dipole moments as for the QD simulations (see Ref. 54 for more details). All XFAIMS results presented below were carried out for an ensemble of 100 XFAIMS runs (unless otherwise stated), whose initial conditions were sampled from a Wigner distribution.

The TSH simulations were performed with the SHARC2.0 suite of programs.[75] We adapted the 'analytical PESs interface' of SHARC2.0 to read the PECs and dipole moments used in the QD and XFAIMS simulations. All TSH results were averaged over 1000 independent trajectories (initial conditions sampled from a Wigner distribution). TSH simulations were carried out on field-adiabatic PECs, unless otherwise stated. We used the commonly-employed energy-difference based correction scheme[76,77] for the decoherence correction, with a standard decoherence parameter of 0.1 a.u.. We did not observe significant variations of the dynamics by changing the value of this parameter. The time step for the propagation was set to 1 a.u., and the velocities were not rescaled upon field-induced hops, as done in XFAIMS.

Results and discussion

The following comparison between XFAIMS and TSH will be based on the photoexcitation and excited-state dynamics of LiH in three different scenarios: (*i*) photoexcitation of LiH from its ground electronic state with an ultrashort 71 a.u. (1.7 fs) UV pulse and study of the subsequent wavepacket dynamics, (*ii*) photoexcitation of LiH from its ground electronic

state with a longer 1175 a.u. (28.4 fs) IR pulse, and (*iii*) photoexcitation of LiH from its ground electronic state with an ultrashort UV pump pulse, followed by a probe of the nuclear wavepackets dynamics after a certain time delay by a second ultrashort UV pulse.

Excitation of LiH with a short UV pulse – role of decoherence

The starting point for our comparison between XFAIMS and TSH is the simple photoexcitation of LiH by an ultrashort UV pulse. The molecule is initially in its ground electronic state S_0 (see inset of Fig. 2) and will interact with a pulse (depicted by a gray curve in Fig. 2) whose central frequency matches the energy gap between S_1 and S_0. The numerically-exact QD dynamics shows that the pulse efficiently promotes 39% of the population to S_1 (red curve in Fig. 2). Despite their respective approximations, both XFAIMS and TSH dynamics lead to a final population in S_1 in close agreement with the QD result – 39% for XFAIMS (blue curve in Fig. 2) and 37% for TSH (orange curve in Fig. 2). Removing the decoherence correction in TSH ('TSH*' in Fig. 2) does not significantly alter the result of the dynamics with an S_1 population of 37% after the pulse. We note that the difference in population trace between TSH and XFAIMS/QD *during* the pulse is related, for this pulse parameters, to the different electronic representation, *i.e.*, field-adiabatic (TSH) vs field-diabatic (XFAIMS and QD). The two basis are, however, identical when the interaction with the pulse is over. The excellent agreement between TSH and QD dynamics obtained in this first test should not come as a surprise[44] – such a short pulse of light leads to a very localized coupling (in time) between S_0 and S_1, a scenario where the underlying approximations of surface hopping have proved successful.

Let us now compare the nuclear probability densities obtained with the different methods after $t = 1250$ a.u. of dynamics (Fig. 3). Fig. 3a shows the nuclear probability densities of QD (red), XFAIMS (blue), and TSH (orange) in S_0 (lower panel) and S_1 (upper panel). The TSH probability density for a given electronic state is obtained in Fig. 3a by histogramming all the trajectories that are running in this particular state at a given time. In other words,

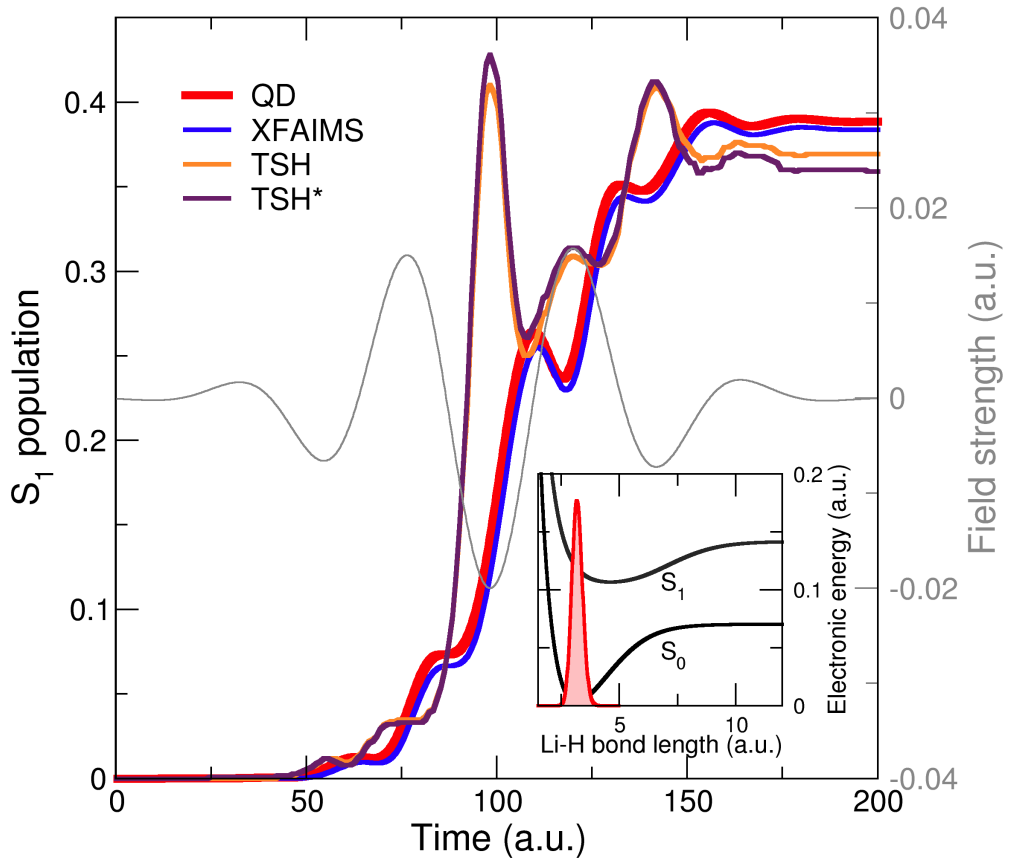

Figure 2: Photoexcitation of LiH with a short UV pulse. The population in the first excited state (S_1) is plotted over time for QD (red curve), XFAIMS (blue curve), TSH with decoherence correction (orange curve), TSH without decoherence correction ('TSH*', palatinate curve). The applied UV pulse is depicted in light gray. The inset shows the potential energy curves for S_0 and S_1 (black), with the initial QD nuclear probability density in the ground electronic state (red).

it is related to the *fraction of trajectories* in an electronic state I, Π_I. Both XFAIMS and TSH probability densities exhibit a similar behavior, with a nuclear probability density in S_1 that has departed from the Franck-Condon region and reached regions of large Li-H bond length, in agreement with the QD simulation. We note that the difference between the XFAIMS and QD nuclear density on S_0 results from the approximations of the former, *i.e.*, a limited number of TBFs (with frozen width) combined with the saddle-point and independent first-generation approximations.[54]

As mentioned earlier, each TSH trajectory is associated with a set of complex amplitudes, one per electronic state. It is therefore informative to generate histograms for these quantities

as well, being critical in the context of the overcoherence problem in TSH. We can achieve this by generating a histogram of all trajectories, but instead of attributing to a given trajectory a value of '1' for its running state and '0' for the other state, we use the actual squared modulus of the complex amplitude for each state to weight each trajectory (such histograms will be related to the *averaged electronic population* in an electronic state I, $\overline{p}_I$). If internal consistency is respected, the two ways of obtaining TSH populations, Π_I and $\overline{p}_I$, should be similar.[76]

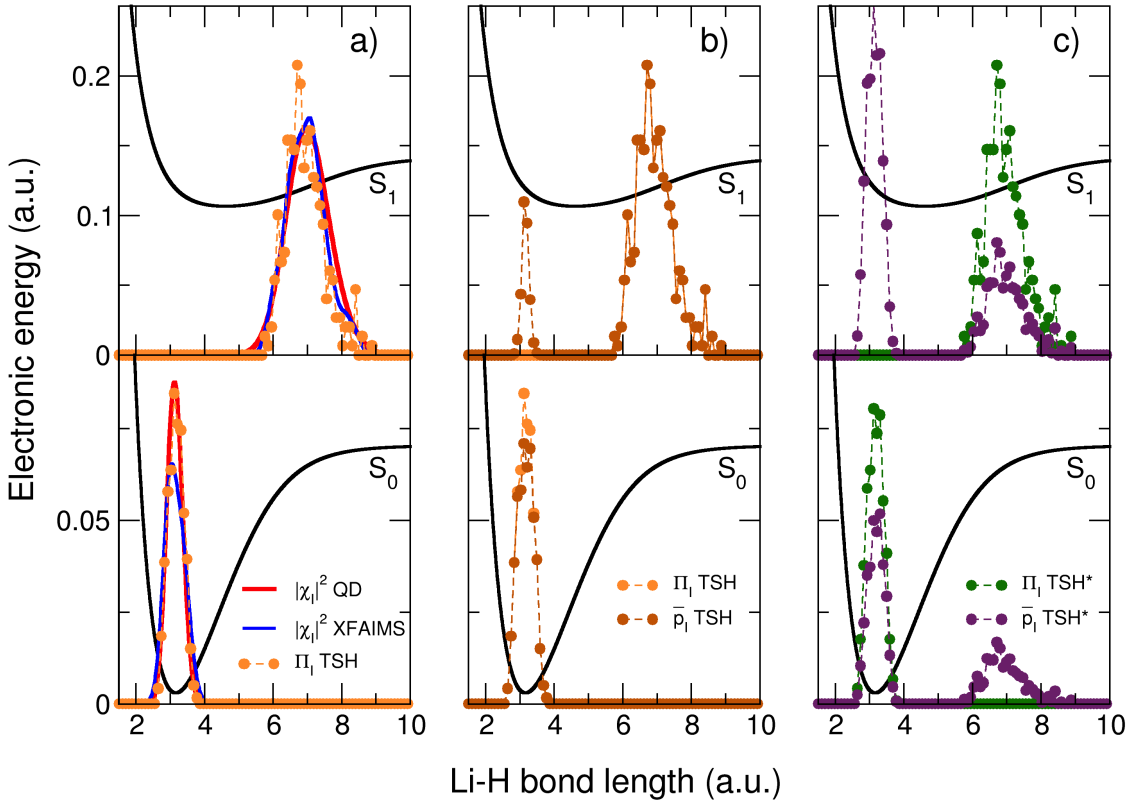

Figure 3: Snapshot of the excited-state dynamics of LiH at $t = 1250$ a.u., when the S_1 nuclear wavepacket has left the Franck-Condon region. Lower (upper) panels show the nuclear probability densities in S_0 (S_1). a) Comparison between the nuclear probability densities produced by QD (red curve), XFAIMS (blue curve), and the trajectory-fraction histograms of TSH with decoherence correction (light-orange dotted curve). b) Comparison between the trajectory-fraction (Π_I, light-orange dotted curve) and the electronic-population ($\overline{p}_I$, dark-orange dotted curve) histograms for TSH with decoherence correction. c) Comparison between the trajectory-fraction (Π_I, green dotted curve) and the electronic-population ($\overline{p}_I$, palatinate dotted curve) histograms for TSH without decoherence correction. See text for more details on the different TSH histograms. All wavepackets/histograms on S_0 (S_1) were divided by a factor 12 (1.5) for clarity.

Let us first compare the two types of histograms for the TSH* dynamics, *i.e.*, TSH without decoherence correction (Fig. 3c, histograms based on the fraction of trajectories are in green, while the ones representing the averaged electronic population are shown in palatinate). A comparison with the previously described histograms based on the fraction of TSH trajectories reveals a striking difference: the $\overline{p}_I$ histograms show more than one peaks per electronic state. For example, the ground-state histogram of TSH* (lower panel of Fig. 3c) would indicate that, after 1250 a.u. of dynamics, the LiH nuclear wavepacket in S_0 should have branched, with a contribution near the Franck-Condon region (around a Li-H bond length of ~ 3.2 a.u.) and another at longer bond length (~ 6.7 a.u.). This observation, though, is the direct result of the overcoherence problem: TSH without correction cannot describe the decoherence between the S_0 and S_1 nuclear wavepackets. Briefly, this lack of decoherence can be understood at the level of a single TSH* as follows: (*i*) the short UV pulse promotes some amplitude, but not all of it, from S_0 to S_1, (*ii*) this amplitude transfer results in a hop of the trajectory to S_1, (*iii*) the trajectory, now evolving in S_1, relaxes away from the Franck-Condon region; however, this specific trajectory still has residual amplitude on the ground state, and this amplitude is forced to follow the trajectory in its dynamics in S_1, giving the artificial result that some S_0 probability density can be found at a Li-H bond length of ~ 6.7 a.u. (lower panel of Fig. 3c). The very same effect can be observed in the lowest excited state (upper panel of Fig. 3c), where TSH* seems to predict that some nuclear probability density would remain in the Franck-Condon region long after the end of the light pulse – a consequence of amplitude transfer between S_0 and S_1 for trajectories that will stay in S_0. Applying a decoherence correction to TSH readily fixes this problem, as attested by the close similarity between the TSH histograms in the Fig. 3b – except for a small deviation in S_1, near the Franck-Condon region.

In summary, the population transfer between S_0 and S_1 upon photoexcitation of LiH with a short UV pulse is well described by all methods tested. While the final electronic-state populations obtained with TSH and TSH* are in good agreement with the QD result, a

more in-depth investigation reveals that a decoherence correction is required to ensure an adequate description of the wavepacket branching. On the other hand, XFAIMS naturally includes the decoherence of the S_0 and S_1 nuclear wavepackets thanks to the use of different (coupled) TBFs for S_0 to S_1, resulting in a close agreement with QD both for the population and the description of the nuclear wavepackets.

Excitation of LiH with a long IR pulse – effect of the independent trajectory approximation

The previous Section has demonstrated that both TSH and XFAIMS describe accurately the transfer of electronic population resulting from the absorption of an ultrashort UV pulse by LiH. Despite the excellent performance of TSH with this short pulse, previous works showed that TSH suffers from its independent trajectory approximation when longer laser pulses (tens to hundreds of femtoseconds) are employed.[44] This failure is particularly dramatic if one considers that ultrafast spectroscopy experiments on molecules are commonly using pulses with such lengths. Therefore, we want to test at this stage whether XFAIMS is capable of reproducing the photoexcitation dynamics triggered by longer laser pulses.

In the following, we describe the electronic transition of LiH triggered by a 1175 a.u. (28.4 fs) IR laser pulse (thin gray curve in Fig. 4). The numerically-exact QD simulation shows an increase of the S_1 population state for the first 2000 a.u. of the dynamics, followed by an overall back transfer of the S_1 population back to S_0 at later times, until the end of the pulse. This overall S_1 population back transfer, observed after 2000 a.u. of dynamics, is due to the motion of the nuclear wavepacket on S_1: upon relaxation from the Franck-Condon region, the S_1 nuclear wavepacket reaches a LiH bond length region where the energy gap between S_0 and S_1 decreases sufficiently (see inset Fig. 2) to match the frequency of the IR pulse, leading to an efficient transfer of S_1 back to S_0.

With the inclusion of a decoherence correction, the S_1 population trace obtained with TSH (orange curve in Fig. 4) matches the QD one qualitatively, but the final population on

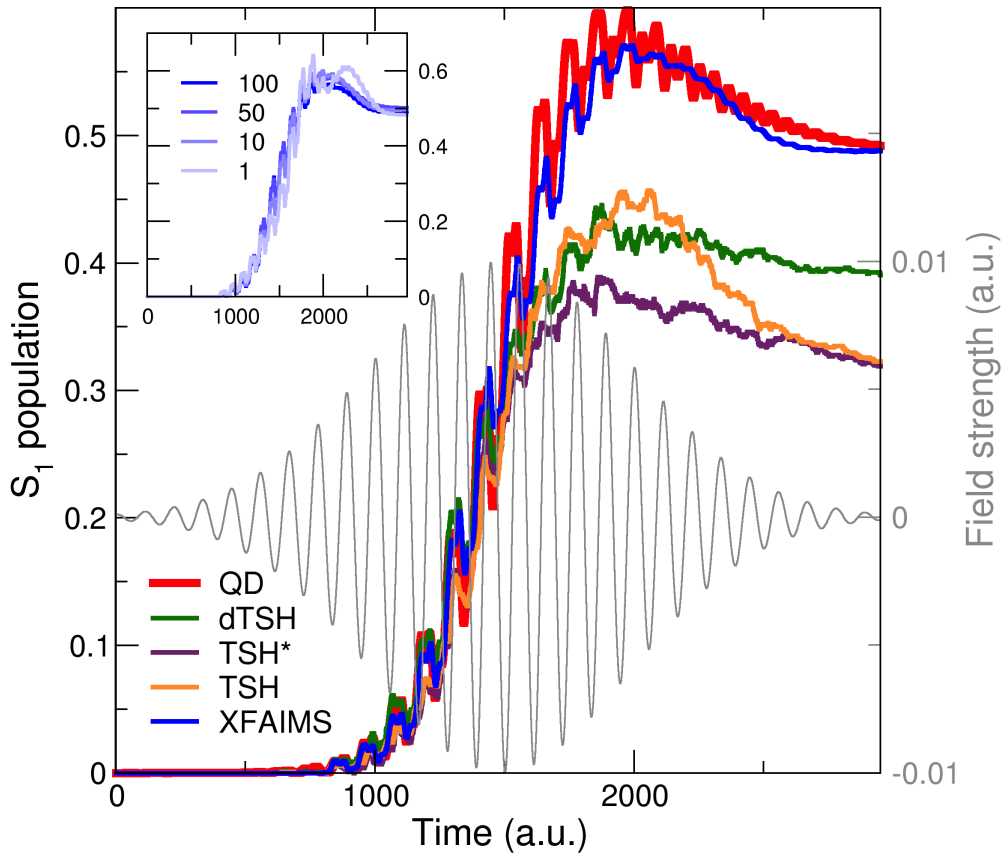

Figure 4: Photoexcitation of LiH with a long IR pulse. The population in the first excited state (S_1) is plotted over time for QD (red curve), XFAIMS (blue curve), TSH with decoherence correction (orange curve), TSH without decoherence correction ('TSH*', palatinate curve), and TSH within field-diabatic representation ('dTSH', green curve). The applied IR pulse is depicted in light gray. The inset depicts the convergence of the XFAIMS S_1 population trace with respect to the number of initial conditions.

S_1 by the end of the pulse deviates significantly from the exact result (0.32 for TSH, 0.49 for QD). Removing the decoherence correction (palatinate curve in Fig. 4) does not alter the TSH result markedly for the first part of the pulse, when the population is transferred from S_0 to S_1. However, the depopulation of S_1 at a later time, resulting from the motion of the S_1 wavepacket away from the Franck-Condon region, suffers from the decoherence problem as expected from the result presented in the previous Section. Hence, the decoherence correction helps describe this specific back transfer process by reducing for each trajectory the overcoherence between its amplitudes (as observed previously by comparing Fig. 3b and Fig. 3c). As mentioned in the Theory Section above, different representations of the

electronic states with respect to the external field are available to perform TSH. In all the previous examples, we used a (field-) adiabatic basis, but TSH can also be employed in a (field-) diabatic way (dTSH). As shown in Fig. 4 (green curve), this different representation leads to a different result for the final S_1 population (0.39), but still deviates from the QD result significantly.

Importantly, these simulations show that the maximum of the TSH S_1 population trace during the photoexcitation, as well as its final value at the end of the pulse, *always* deviate from the QD result, independently of the use of decoherence correction or a different representation. This observation highlights the fact that the excitation of LiH with long pulses strongly stresses the independent trajectory approximation underlying TSH. While a consequence of this approximation – the overcoherence of TSH trajectories – can be partially fixed by applying a correction, there is no simple cure for the lack of correlation between the trajectories which is deeply rooted in the TSH strategy. Interactions between trajectories would, however, be necessary to gain access to the description of the complex interplay between the S_0 and S_1 nuclear wavepackets during the long photoexcitation process, nonlocal by nature. It is precisely where one would expect XFAIMS to outperform TSH, as it uses coupled TBFs.

Despite its inherent approximations, XFAIMS (blue curve in Fig. 4) reproduces quantitatively the QD population trace, both during and at the end of the pulse. In particular, XFAIMS accurately captures the back transfer of population to S_0 upon relaxation of the nuclear wavepacket in S_1. But achieving this result comes at a cost: one initial condition – consisting of a single TBF in S_0 at time $t = 0$ – will spawn in average 14.6 TBFs on S_1, which in turn spawn an additional 4.4 TBFs back in S_0. All these TBFs are coupled, in stark contrast with the independent trajectories of TSH. This coupling ensures a proper description of the S_1 and S_0 nuclear wavepackets and their dynamics, both being critical to capture the physics of the overall population transfer. As shown in the inset of Fig. 4, a single initial condition (leading to the generation of 22 TBFs) already captures correctly the

physics of this photoexcitation and leads to a final S_1 population in better agreement with QD than TSH (the latter uses 1000 trajectories). Upon averaging over different XFAIMS initial conditions, the S_1 population trace is rapidly refined to mimic the QD one closely. We note that, formally, the number of electronic-structure calculations required per (XF)AIMS integration time step is $\frac{N_{TBFs}(t)\times(N_{TBFs}(t)+1)}{2}$, with $N_{TBFs}(t)$ the number of TBFs at time t.[10] In practice, this number can be substantially reduced by computing couplings only between TBFs that have a substantial overlap.[78] This computational overhead for (XF)AIMS is the price to pay for preserving the couplings between TBFs and bypassing the independent trajectory approximation of TSH. Nevertheless, it is important to realise that the number of initial conditions required to converge the calculation of a given quantity within (XF)AIMS is usually smaller than with TSH – as exemplified in this Section – as no stochastic process needs to be converged within an (XF)AIMS run.

In silico pump-probe experiment on LiH

In the previous Section, we have shown that coupling TBFs is required to accurately simulate processes where the (nonlocal) interaction between nuclear wavepackets, mediated by an external field, plays a central role. To further test the quality of XFAIMS to describe such processes, we propose here to study an *in silico* pump-probe experiment on LiH (schematically depicted in the inset of Fig. 5).[54,79,80] A first ultrashort UV pump pulse is sent on the molecule ('A' in the inset of Fig. 5), promoting part of the nuclear population from S_0 to S_1. The nuclear wavepacket formed on S_1 will leave the Franck-Condon region towards longer LiH bond length, before eventually bouncing back ('B' in the inset of Fig. 5). After a certain time delay, an ultrashort UV probe pulse is sent on the molecule, triggering a new population transfer between the two electronic states ('C' in the inset of Fig. 5). In this experiment, the final population after the two pulses will be influenced heavily by the interaction between the two nuclear wavepackets, depending on their overlap and phase difference. Hence, this last test probes in an even more stringent way the approximations of TSH and XFAIMS, as

it requires a proper description of the photoexcitation process, the separation and dynamics of the nuclear wavepackets on S_0 and S_1, and their interferences at a later time when the second pulse hits the molecule. Varying the time delay between the pump and the probe pulses produces oscillations in the final S_1 population that reveal the electronic beating between the nuclear wavepackets on S_0 and S_1, as shown for the numerically exact QD simulations (red curve in Fig. 5). For short time delays between the pulses (2500-2750 a.u.), the nuclear

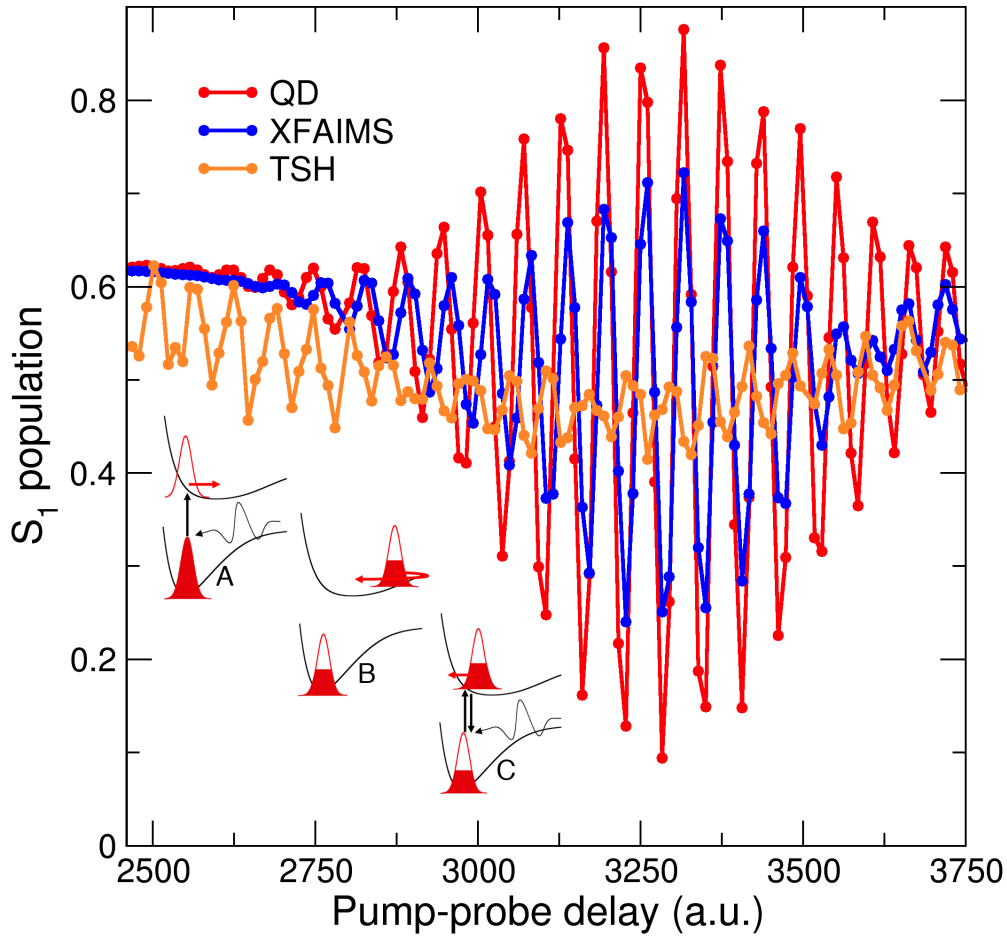

Figure 5: Pump-probe experiment on LiH. Evolution of the final S_1 population as a function of the pump-probe time delay for QD (red curve), XFAIMS (blue curve), and TSH with decoherence correction (orange curve). The inset shows the three steps of the experiment: pump pulse (A), evolution of the system (B), probe pulse after a certain time delay (C).

wavepacket on S_1 does not have enough time to come back in the Franck-Condon region, leading to a weak interaction with the S_0 wavepacket and small variations of the final S_1 population as a function of the delay. At longer delay times, the S_1 nuclear wavepacket

is close enough to the Franck-Condon region to interact with the S_0 wavepacket, and the occurrence of fine interferences between them is attested by the large oscillations of the final population for small variations of the time delay. Unsurprisingly, TSH does not capture the oscillations of the final S_1 population (orange curve in Fig. 5). A TSH trajectory can describe the dynamics of the nuclear wavepacket in S_1 *or* in S_0, but the independent trajectory approximation prevents the TSH trajectories to describe the simultaneous dynamics of the S_1 and S_0 nuclear wavepackets – a feature required to *accurately* reproduce the trends in oscillations observed for different time delays. For a TSH trajectory evolving in S_1, the decoherence correction of TSH might bring its S_0 amplitude to zero after hopping, preventing a coherent interaction between the two amplitudes when the second pulse reaches the molecule. If one looks at the same trajectory, but this time without a decoherence correction, an S_0 TSH amplitude would be artificially propagated along the (S_1) TSH trajectory and both amplitudes could interact due to the second pulse; however, the overcoherence of TSH amplitudes means that the influence of the overlap between the S_1 and S_0 nuclear wavepackets would be missed. As such, the independent trajectory approximation makes the pump-probe experiment challenging for TSH, with and without decoherence correction.

Au contraire, the use of coupled TBFs allows XFAIMS to capture the oscillation in the S_1 population qualitatively (blue curve in Fig. 5). The reason why XFAIMS does not reproduce the final S_1 population quantitatively for such pump-probe experiment is related to its underlying approximations – a proper description of the overlap between nuclear wavepackets would require to relax the independent first generation approximation – and was explained in detail in Ref. 54. Nevertheless, this example shows that XFAIMS can capture at least qualitatively the physics underlying such pump-probe experiment, and improves over the description offered by TSH.

Conclusion

In this work, we validated the use of XFAIMS for the study of pulse-triggered excited-state dynamics. In particular, we showed that XFAIMS could capture the transfer of electronic population at least qualitatively for challenging excitation processes of LiH involving long pulses or pump/probe pulse sequences – cases that are notoriously challenging for the approximations of TSH. The independent trajectory approximation inherent to the TSH dynamics hampers a proper description of the complex interplay between nuclear wavepacket dynamics on the electronic states coupled by the laser pulse. More generally, the tests presented in this work exemplify the difficulty experienced by TSH in describing quantum coherence and decoherence processes taking place when nuclear wavepackets evolving on different electronic states interfere after being separated. While certain issues related to the overcoherence of TSH trajectories can be fixed by applying an ad hoc decoherence correction, the interaction between the nuclear wavepackets and their mutual dynamics can only be adequately captured by restoring a coupling between the trajectories. These issues are naturally addressed in XFAIMS by using coupled TBFs, as attested by the good performance of this method, and despite its underlying approximations. Hence, XFAIMS appears to be a reliable and more robust alternative to TSH for the explicit simulation of light-triggered excited-state processes in molecular systems.

Acknowledgement

B.M. acknowledges support from the Fonds National de la Recherche Scientifique, Belgium (F.R.S.-FNRS), and the University of Liège. Computational resources have been provided by the Consortium des Equipements de Calcul Intensif (CECI), funded by the F.R.S.-FNRS under Grant No. 2.5020.11. B.F.E.C. acknowledges support from Durham University.

References

(1) Tully, J. C. Perspective: Nonadiabatic dynamics theory. *J. Chem. Phys.* **2012**, *137*, 22A301.

(2) Yarkony, D. Nonadiabatic Quantum Chemistry: Past, Present, and Future. *Chem. Rev.* **2012**, *112*, 481.

(3) Domcke, W., Yarkony, D., Köppel, H., Eds. *Conical Intersections: Theory, Computation and Experiment*; World Scientific Pub Co Inc, 2012; Vol. 17.

(4) Tannor, D. J. *Introduction to quantum mechanics, a time-dependent perspective*; University Science Books: Sausalito, California, 2007.

(5) Persico, M.; Granucci, G. *Photochemistry: A Modern Theoretical Perspective*; Springer, 2018.

(6) Suchan, J.; Hollas, D.; Curchod, B. F. E.; Slavicek, P. On the Importance of Initial Conditions for Excited-State Dynamics. *Faraday Discuss.* **2018**, *212*, 307–330.

(7) Beck, M. H.; Jäckle, A.; Worth, G. A.; Meyer, H. D. The multiconfiguration time-dependent Hartree (MCTDH) method: a highly efficient algorithm for propagating wavepackets. *Phys. Rep.* **2000**, *324*, 1–105.

(8) Worth, G. A.; Meyer, H. D.; Cederbaum, L. S. In *Conical Intersections: Electronic Structure, Dynamics & Spectroscopy*; Domcke, W., Yarkony, D. R., Köppel, H., Eds.; Advanced Series in Physical Chemistry; 2004; Vol. 15; Chapter 14, pp 583–617.

(9) Meyer, H.-D.; Gatti, F.; Worth, G. A. *Multidimensional quantum dynamics*; John Wiley & Sons, 2009.

(10) Curchod, B. F. E.; Martínez, T. J. Ab initio nonadiabatic quantum molecular dynamics. *Chem. Rev.* **2018**, *118*, 3305–3336.

(11) Worth, G.; Robb, M.; Burghardt, I. A novel algorithm for non-adiabatic direct dynamics using variational Gaussian wavepackets. *Faraday Discuss.* **2004**, *127*, 307–323.

(12) Lasorne, B.; Bearpark, M. J.; Robb, M. A.; Worth, G. A. Direct quantum dynamics using variational multi-configuration Gaussian wavepackets. *Chem. Phys. Lett.* **2006**, *432*, 604–609.

(13) Lasorne, B.; Robb, M.; Worth, G. Direct quantum dynamics using variational multi-configuration Gaussian wavepackets. Implementation details and test case. *Phys. Chem. Chem. Phys.* **2007**, *9*, 3210–3227.

(14) Worth, G. A.; Robb, M. A.; Lasorne, B. Solving the time-dependent Schrödinger equation for nuclear motion in one step: direct dynamics of non-adiabatic systems. *Mol. Phys.* **2008**, *106*, 2077–2091.

(15) Mendive-Tapia, D.; Lasorne, B.; Worth, G. A.; Robb, M. A.; Bearpark, M. J. Towards converging non-adiabatic direct dynamics calculations using frozen-width variational Gaussian product basis functions. *J. Chem. Phys.* **2012**, *137*, 22A548.

(16) Richings, G.; Polyak, I.; Spinlove, K.; Worth, G.; Burghardt, I.; Lasorne, B. Quantum dynamics simulations using Gaussian wavepackets: the vMCG method. *Int. Rev. Phys. Chem.* **2015**, *34*, 269–308.

(17) Shalashilin, D. Quantum mechanics with the basis set guided by Ehrenfest trajectories: Theory and application to spin-boson model. *J. Chem. Phys.* **2009**, *130*, 244101.

(18) Shalashilin, D. V. Nonadiabatic dynamics with the help of multiconfigurational Ehrenfest method: Improved theory and fully quantum 24D simulation of pyrazine. *J. Chem. Phys.* **2010**, *132*, 244111.

(19) Saita, K.; Shalashilin, D. V. On-the-fly ab initio molecular dynamics with multiconfigurational Ehrenfest method. *J. Chem. Phys.* **2012**, *137*, 22A506.

(20) Makhov, D.; Symonds, C.; Fernandez-Alberti, S.; Shalashilin, D. Ab initio quantum direct dynamics simulations of ultrafast photochemistry with Multiconfigurational Ehrenfest approach. *Chem. Phys.* **2017**, *493*, 200–218.

(21) Martínez, T. J.; Ben-Nun, M.; Levine, R. D. Multi-electronic-state molecular dynamics: A wave function approach with applications. *J. Phys. Chem.* **1996**, *100*, 7884–7895.

(22) Martínez, T. J.; Levine, R. D. Non-adiabatic molecular dynamics: Split-operator multiple spawning with applications to photodissociation. *J. Chem. Soc., Faraday Trans.* **1997**, *93*, 941–947.

(23) Ben-Nun, M.; Martínez, T. J. Nonadiabatic molecular dynamics: Validation of the multiple spawning method for a multidimensional problem. *J. Chem. Phys.* **1998**, *108*, 7244–7257.

(24) Ben-Nun, M.; Quenneville, J.; Martínez, T. J. Ab initio multiple spawning: Photochemistry from first principles quantum molecular dynamics. *J. Phys. Chem. A* **2000**, *104*, 5161–5175.

(25) Hack, M. D.; Wensmann, A. M.; Truhlar, D. G.; Ben-Nun, M.; Martínez, T. J. Comparison of full multiple spawning, trajectory surface hopping, and converged quantum mechanics for electronically nonadiabatic dynamics. *J. Chem. Phys.* **2001**, *115*, 1172.

(26) Ben-Nun, M.; Martínez, T. J. Ab Initio Quantum Molecular Dynamics. *Adv. Chem. Phys.* **2002**, *121*, 439–512.

(27) Virshup, A. M.; Punwong, C.; Pogorelov, T. V.; Lindquist, B. A.; Ko, C.; Martinez, T. J. Photodynamics in Complex Environments: Ab Initio Multiple Spawning Quantum Mechanical/Molecular Mechanical Dynamics. *J. Phys. Chem. B* **2008**, *113*, 3280–3291.

(28) Tully, J. C. Mixed quantum classical dynamics. *Faraday Discuss.* **1998**, *110*, 407.

(29) Crespo-Otero, R.; Barbatti, M. Recent Advances and Perspectives on Nonadiabatic Mixed Quantum–Classical Dynamics. *Chem. Rev.* **2018**, *118*, 7026–7068.

(30) Bjerre, A.; Nikitin, E. Energy transfer in collisions of an excited sodium atom with a nitrogen molecule. *Chem. Phys. Lett.* **1967**, *1*, 179–181.

(31) Tully, J. C.; Preston, R. K. Trajectory Surface Hopping Approach to Nonadiabatic Molecular Collisions: The Reaction of H^+ with D_2. *J. Chem. Phys.* **1971**, *55*, 562–572.

(32) Tully, J. C. Molecular dynamics with electronic transitions. *J. Chem. Phys.* **1990**, *93*, 1061–1071.

(33) Delos, J. B.; Thorson, W. R.; Knudson, S. K. Semiclassical theory of inelastic collisions. I. Classical picture and semiclassical formulation. *Phys. Rev. A* **1972**, *6*, 709.

(34) Yonehara, T.; Hanasaki, K.; Takatsuka, K. Fundamental Approaches to Nonadiabaticity: Toward a Chemical Theory beyond the Born-Oppenheimer Paradigm. *Chem. Rev.* **2012**, *112*, 499–542.

(35) Min, S. K.; Agostini, F.; Gross, E. K. Coupled-trajectory quantum-classical approach to electronic decoherence in nonadiabatic processes. *Phys. Rev. Lett.* **2015**, *115*, 073001.

(36) Agostini, F.; Min, S. K.; Abedi, A.; Gross, E. Quantum-Classical Nonadiabatic Dynamics: Coupled-vs Independent-Trajectory Methods. *J. Chem. Theory Comput.* **2016**, *12*, 2127–2143.

(37) Min, S. K.; Agostini, F.; Tavernelli, I.; Gross, E. K. Ab initio nonadiabatic dynamics with coupled trajectories: A rigorous approach to quantum (de) coherence. *J. Phys. Chem. Lett.* **2017**, *8*, 3048–3055.

(38) Curchod, B. F. E.; Agostini, F.; Tavernelli, I. CT-MQC–a coupled-trajectory mixed quantum/classical method including nonadiabatic quantum coherence effects. *Eur. Phys. J. B* **2018**, *91*, 168.

(39) Jones, G. A.; Acocella, A.; Zerbetto, F. On-the-Fly, Electric-Field-Driven, Coupled Electron- Nuclear Dynamics. *J. Phys. Chem. A* **2008**, *112*, 9650–9656.

(40) Mitrić, R.; Petersen, J.; Bonačić-Koutecký, V. Laser-field-induced surface-hopping method for the simulation and control of ultrafast photodynamics. *Phys. Rev. A* **2009**, *79*, 053416.

(41) Marquetand, P.; Richter, M.; González-Vázquez, J.; Sola, I.; González, L. Nonadiabatic ab initio molecular dynamics including spin-orbit coupling and laser fields. *Faraday Discuss.* **2011**, *153*, 261–273.

(42) Tavernelli, I.; Curchod, B. F. E.; Rothlisberger, U. Mixed quantum-classical dynamics with time-dependent external fields: A time-dependent density-functional-theory approach. *Phys. Rev. A* **2010**, *81*, 052508.

(43) Curchod, B. F. E.; Penfold, T. J.; Rothlisberger, U.; Tavernelli, I. Local control theory in trajectory-based nonadiabatic dynamics. *Phys. Rev. A* **2011**, *84*, 042507.

(44) Bajo, J. J.; Granucci, G.; Persico, M. Interplay of radiative and nonradiative transitions in surface hopping with radiation-molecule interactions. *J. Chem. Phys.* **2014**, *140*, 044113.

(45) Persico, M.; Granucci, G. An overview of nonadiabatic dynamics simulations methods, with focus on the direct approach versus the fitting of potential energy surfaces. *Theor. Chem. Acc.* **2014**, *133*, 1–28.

(46) Curchod, B. F.; Penfold, T. J.; Rothlisberger, U.; Tavernelli, I. Local Control Theory in Trajectory Surface Hopping Dynamics Applied to the Excited-State Proton Transfer of 4-Hydroxyacridine. *ChemPhysChem* **2015**, *16*, 2127–2133.

(47) Fiedlschuster, T.; Handt, J.; Gross, E.; Schmidt, R. Surface hopping in laser-driven molecular dynamics. *Phys. Rev. A* **2017**, *95*, 063424.

(48) Yagi, K.; Takatsuka, K. Nonadiabatic chemical dynamics in an intense laser field: electronic wave packet coupled with classical nuclear motions. *J. Chem. Phys.* **2005**, *123*, 224103.

(49) Kim, J.; Tao, H.; White, J. L.; Petrovic, V. S.; Martinez, T. J.; Bucksbaum, P. H. Control of 1,3-cyclohexadiene photoisomerization using light-induced conical intersections. *J. Phys. Chem. A* **2011**, *116*, 2758–2763.

(50) Kim, J.; Tao, H.; Martinez, T. J.; Bucksbaum, P. Ab initio multiple spawning on laser-dressed states: a study of 1,3-cyclohexadiene photoisomerization via light-induced conical intersections. *J. Phys. B* **2015**, *48*, 164003.

(51) Mignolet, B.; Curchod, B. F. E.; Martínez, T. J. Communication: XFAIMS—eXternal Field Ab Initio Multiple Spawning for electron-nuclear dynamics triggered by short laser pulses. *J. Chem. Phys.* **2016**, *145*, 191104.

(52) Makhov, D. V.; Shalashilin, D. V. Floque Hamiltonian for incorporating electronic excitation by a laser pulse into simulations of non-adiabatic dynamics. *Chem. Phys.* **2018**, *515*, 46–51.

(53) Mignolet, B.; Curchod, B. F. E.; Remacle, F.; Martínez, T. J. Sub-Femtosecond Stark Control of Molecular Photoexcitation With Near Single-Cycle Pulses. *J. Phys. Chem. Lett.* **2019**, *10.1021/acs.jpclett.8b03814*.

(54) Mignolet, B.; Curchod, B. F. E. A walk through the approximations of ab initio multiple spawning. *J. Chem. Phys.* **2018**, *148*, 134110.

(55) Curchod, B. F. E.; Tavernelli, I. On trajectory-based nonadiabatic dynamics: Bohmian dynamics versus trajectory surface hopping. *J. Chem. Phys.* **2013**, *138*, 184112.

(56) Subotnik, J. E.; Ouyang, W.; Landry, B. R. Can we derive Tully's surface-hopping

algorithm from the semiclassical quantum Liouville equation? Almost, but only with decoherence. *J. Chem. Phys.* **2013**, *139*, 214107.

(57) Barbatti, M. Nonadiabatic dynamics with trajectory surface hopping method. *WIREs Comput. Mol. Sci.* **2011**, *1*, 620–633.

(58) Jasper, A. W.; Nangia, S.; Zhu, C.; Truhlar, D. G. Non-Born-Oppenheimer Molecular Dynamics. *Acc. Chem. Res.* **2006**, *39*, 101.

(59) Granucci, G.; Persico, M. Critical appraisal of the fewest switches algorithm for surface hopping. *J. Chem. Phys.* **2007**, *126*, 134114.

(60) Jaeger, H. M.; Fischer, S.; Prezhdo, O. V. Decoherence-induced surface hopping. *J. Chem. Phys.* **2012**, *137*, 22A545.

(61) Subotnik, J. E.; Ouyang, W.; Landry, B. R. Can we derive Tully's surface-hopping algorithm from the semiclassical quantum Liouville equation? Almost, but only with decoherence. *J. Chem. Phys.* **2013**, *139*, 214107.

(62) Gao, X.; Thiel, W. Non-Hermitian surface hopping. *Phys. Rev. E* **2017**, *95*, 013308.

(63) Bittner, E. R.; Rossky, P. J. Quantum decoherence in mixed quantum-classical systems: Nonadiabatic processes. *J. Chem. Phys.* **1995**, *103*, 8130–8143.

(64) Fang, J.-Y.; Hammes-Schiffer, S. Improvement of the Internal Consistency in Trajectory Surface Hopping. *J. Phys. Chem. A* **1999**, *103*, 9399–9407.

(65) Shenvi, N.; Subotnik, J. E.; Yang, W. Simultaneous-trajectory surface hopping: A parameter-free algorithm for implementing decoherence in nonadiabatic dynamics. *J. Chem. Phys.* **2011**, *134*, 144102.

(66) Shenvi, N.; Subotnik, J. E.; Yang, W. Phase-corrected surface hopping: Correcting the phase evolution of the electronic wavefunction. *J. Chem. Phys.* **2011**, *135*, 024101.

(67) Shenvi, N.; Yang, W. Achieving partial decoherence in surface hopping through phase correction. *J. Chem. Phys.* **2012**, *137*, 22A528.

(68) Subotnik, J. E.; Shenvi, N. A new approach to decoherence and momentum rescaling in the surface hopping algorithm. *J. Chem. Phys.* **2011**, *134*, 024105.

(69) Subotnik, J. E.; Shenvi, N. Decoherence and surface hopping: When can averaging over initial conditions help capture the effects of wave packet separation? *J. Chem. Phys.* **2011**, *134*, 244114.

(70) Jasper, A. W.; Truhlar, D. G. Electronic decoherence time for non-Born-Oppenheimer trajectories. *J. Chem. Phys.* **2007**, *127*, 194306.

(71) Thachuk, M.; Ivanov, M. Y.; Wardlaw, D. M. A semiclassical approach to intense-field above-threshold dissociation in the long wavelength limit. *J. Chem. Phys.* **1996**, *105*, 4094–4104.

(72) Richter, M.; Marquetand, P.; González-Vázquez, J.; Sola, I.; González, L. SHARC: ab Initio Molecular Dynamics with Surface Hopping in the Adiabatic Representation Including Arbitrary Couplings. *J. Chem. Theory Comput.* **2011**, *7*, 1253–1258.

(73) Bajo, J.; González-Vázquez, J.; Sola, I.; Santamaria, J.; Richter, M.; Marquetand, P.; González, L. Mixed Quantum-Classical Dynamics in the Adiabatic Representation to Simulate Molecules Driven by Strong Laser Pulses. *J. Phys. Chem. A* **2012**, *16*, 2800.

(74) Mai, S.; Marquetand, P.; González, L. Nonadiabatic dynamics: The SHARC approach. *WIREs Comput. Mol. Sci.* **2018**, e1370.

(75) Mai, S.; Richter, M.; Heindl, M.; Menger, M. F. S. J.; Atkins, A. J.; Ruckenbauer, M.; Plasser, F.; Oppel, M.; Marquetand, P.; González, L. SHARC2.0: Surface Hopping Including Arbitrary Couplings – Program Package for Non-Adiabatic Dynamics. sharc-md.org, 2018.

(76) Granucci, G.; Persico, M. Critical appraisal of the fewest switches algorithm for surface hopping. *J. Chem. Phys.* **2007**, *126*, 134114–11.

(77) Granucci, G.; Persico, M.; Zoccante, A. Including quantum decoherence in surface hopping. *J. Chem. Phys.* **2010**, *133*, 134111.

(78) Levine, B. G.; Coe, J. D.; Virshup, A. M.; Martinez, T. J. Implementation of ab initio multiple spawning in the Molpro quantum chemistry package. *Chemical Physics* **2008**, *347*, 3–16.

(79) Nikodem, A.; Levine, R.; Remacle, F. Quantum nuclear dynamics pumped and probed by ultrafast polarization controlled steering of a coherent electronic state in LiH. *J. Phys. Chem. A* **2016**, *120*, 3343–3352.

(80) Nikodem, A.; Levine, R.; Remacle, F. Spatial and temporal control of populations, branching ratios, and electronic coherences in LiH by a single one-cycle infrared pulse. *Phys. Rev. A* **2017**, *95*, 053404.

TOC Graphic

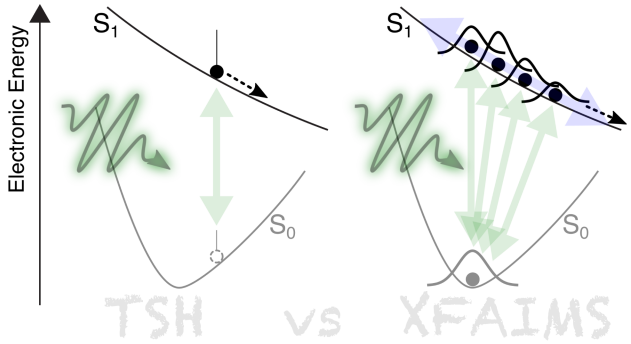

Biography

Basile F. E. Curchod was born in Vevey (Switzerland). He received his PhD in 2013 from the Ecole Polytechnique Fédérale de Lausanne (EPFL, Switzerland), under the direction of Dr. Ivano Tavernelli and co-direction of Prof. Ursula Roethlisberger. After a short stay in the laboratory of Prof. Clémence Corminboeuf (EPFL), he was awarded a Swiss Early.PostDoc grant to join in 2014 the group of Prof. Todd J. Martínez at Stanford University (USA). In December 2015, he began a short postdoctoral stay in the Theory Group directed by Prof. Eberhard K. U. Gross, at the Max Planck Institute in Halle (Germany). In May 2016, he joined the Centre for Computational Chemistry at the University of Bristol (UK) as a Marie Skłodowska-Curie Fellow, working with Dr. David R. Glowacki. In November

2017, he became Assistant Professor in Theoretical Chemistry at Durham University (UK) and secured in September 2018 an ERC Starting Grant. Basile's research focuses on the development and application of theoretical methods to simulate the dynamics of molecules beyond the Born-Oppenheimer approximation (`www.in-silico-photochem.com`).